ELSEVIER Solar Energy Materials and Solar Cells 44 (1996) 177–190

Solar Energy Materials and Solar Cells

Characterization of etching procedure in preparation of CdTe solar cells

Juha Sarlund [a], Mikko Ritala [a,*], Markku Leskelä [a], Eija Siponmaa [b], Riitta Zilliacus [c]

[a] *Department of Chemistry, University of Helsinki, P.O.Box 55, FIN-00014 Helsinki, Finland*
[b] *Microchemistry Ltd, P.O.Box 45, FIN-02151 Espoo, Finland*
[c] *Technical Research Centre of Finland, VTT Chemical Technology, P.O. Box 1404, FIN-02044 Espoo, Finland*

Received 7 February 1996; accepted 2 May 1996

Abstract

An etching procedure for forming a low resistance contact to polycrystalline CdTe thin films in CdS/CdTe solar cells was studied. The etching solution used was a mixture of HNO_3, H_3PO_4 and H_2O. X-ray diffraction (XRD), secondary ion mass spectrometry (SIMS) and electric measurements revealed that the etching results in a formation of crystalline tellurium on the film surface, thereby increasing substantially the conductivity of the surface layer. The total process was found to consist of three steps: (i) immediately after an immersion into the etching solution there was a certain induction period with no discernible changes, (ii) a subsequent reaction step during which poorly crystallized elemental tellurium was formed, gaseous byproducts liberated and the surface changed its colour, and (iii) after taking out of the etching solution the tellurium crystallized causing a strong decrease in the sheet resistance. In situ XRD and electric measurements were carried out to follow the third step. The chemical aspects of the three steps as well as their contributions to the reproducibility and control of the overall etching procedure have been considered.

Keywords: Cadmium telluride CdTe; CdTe solar cells; Electrical contracts; Etching; X-ray diffraction

1. Introduction

Owing to its direct bandgap of 1.45 eV ideal for solar energy conversion, CdTe based thin film solar cells have been extensively studied [1,2]. With the best small area

* Corresponding author. Fax: 358 9 191 40198.

PII S0927-0248(96)00053-0

CdS/CdTe heterojunction cells conversion efficiencies exceeding 15% have been achieved. The major problems met in the CdTe solar cell development have been the difficulty of doping and achievement of stable low resistance ohmic contacts to p-type CdTe [1–4]. One common approach to forming low resistance contacts to CdTe is to modify the CdTe surface with certain etches which leave a tellurium film or at least a tellurium rich layer on the CdTe surface and, thereby, lower the resistivity of the surface layer [1,3]. One of these etches is the HNO_3–H_3PO_4–H_2O mixture introduced by Tyan [5]. This etch has been used, for example, in Microchemistry Ltd in preparing stable CdS/CdTe cells with about 12% conversion efficiencies. In practise, however, it has turned out that this etching procedure suffers somewhat from problems related to its reproducibility. The control of the etching process is further complicated by the changes which take place on the CdTe surface still well after that the sample has been taken out of the etching solution. The aim of the present study was to improve the control of the etching procedure by deepening the insight into the chemical and physical processes which take place both during the etching and, importantly, after it.

2. Experimental

The samples studied consisted of a structure: glass/SnO_2:F (500 nm)/CdS (150 nm)/CdTe (3000 nm). The transparent conductor SnO_2:F was of a commercial origin while the CdS and CdTe layers were grown by Atomic Layer Epitaxy as described in references [6] and [7]. After the CdTe deposition most of the samples were heat treated with $CdCl_2$ at 400°C for 20 min to improve their crystallinity [2,8,9].

The standard etching solution consisted of a mixture of 65% HNO_3, 85% H_3PO_4 and H_2O in a volume ratio of 1:71:29. In addition, alternative etching solutions whose compositions will be described below were also examined. The etching was accomplished simply by immersing the sample into the solution. After etching the samples were washed in distilled water in an ultrasonic bath for 2 min, carefully rinsed with water and blown dry with nitrogen.

The film crystallinity was analyzed with a Philips MPD 1880 powder X-ray diffractometer using CuKα radiation. The elemental depth profiles were measured by using secondary ion mass spectrometry (SIMS). The measurements were carried out on a VG IX70S double focusing magnetic sector instrument. The O_2^+ ions of 5 keV energy were used for the analysis. The ion beam current used was 3 nA and the beam was rastered over an area of 680×1200 μm^2. The followed secondary ions were ^{110}Cd and ^{125}Te. The sputtering rate was determined by sputtering through the whole CdTe film with a known thickness.

Changes in surface conductivity were checked qualitatively with a standard ohmmeter. The exact sheet resistances were measured with the well known four point probe technique. To study in situ how the conductivity changed after the sample had been taken out of the etching solution, a rugged measuring system was constructed. This system consisted of two cantilevers with sharp tips enabling a formation of fixed contact between the tips and the sample surface. The resistance between the two tips was measured with a standard ohmmeter. By using thin film samples with known sheet

resistances it was verified that the readings of this measuring system give a good correlation, in a log–log scale, to the real sheet resistances, thereby validating its use in following the changes in the sheet resistances. The major advantage of using this rugged measuring system was that it could also be operated in an oven at elevated temperatures.

3. Results

3.1. Visual inspection of the etching process

In order to gain a preliminary insight into the etching process, it was first inspected visually with an optical microscope. The standard HNO_3–H_3PO_4–H_2O etching solution described above was used. Before etching the CdTe surface was dark grey and its surface resistivity was too high to be measured either with a four point probe having an upper limit of 2×10^7 $\Omega/\square$ or with a standard ohmmeter. Immediately after immersion into the etching solution no changes could be seen. After a certain period, a length of which varied from sample to sample in a range of 10–15 s, in some cases even 20 s, small bubbles were formed on the film surface. These bubbles, being indicative of a formation of gaseous etching byproducts, grew as the etching proceeded and came visible to the naked eye about 1–2 s after their appearance in the microscope. A part of the bubbles remained attached on the surface during the whole etching procedure which is obviously due to the viscosity of the etching solution.

A few seconds after the appearance of the bubbles in the microscope, i.e., at about the same time as the bubbles became visible to the naked eye, the film surface started to change its colour. First some small islands with a silvery grey colour were formed. These islands expanded rapidly, became into contact with each other and eventually covered the whole surface. The complete change of colour from the dark grey to the silvery grey took place within a few seconds.

In this standard etching procedure the sample was taken out of the solution after 50 s immersion. As it will be described in more detail below, the sheet resistances stabilized only about 30 min after the etching procedure. The sheet resistances measured after an adequate stabilization time were typically within a range of 4–20 $k\Omega/\square$ for this standard etching procedure.

Repetition of the above experiment with different samples revealed that the only major difference was the moment of time when the bubbles appeared. This variation was attributed to the thickness of the oxidized layer on the CdTe surface which, in turn, evidently depends on the sample history. It is worth noting that the etching of CdTe samples which had not undergone the $CdCl_2$ treatment proceeded essentially in a similar manner as that described above for the $CdCl_2$ treated samples.

In some cases the etching procedure was interrupted at that very moment when the bubbles appeared in the microscope, i.e., before the surface changed its colour. As compared with the samples etched normally, the sheet resistances of these incompletely etched samples saturated slower and remained higher, typically 70–120 $k\Omega/\square$. However, the sheet resistances of the incompletely etched samples could be lowered to

30–60 kΩ/□ by heating them for 5 min at 110°C in air immediately after the etching procedure.

3.2. Identification of the etching products

Depth profiling SIMS analysis revealed that during the etching the sample surface had become enriched in Te (Fig. 1). With increasing depth the Cd/Te ratio increased gradually until the bulk value was attained. The total thickness of the Te enriched surface layer increased with increasing etching time being about 300 nm in the 20 s etched sample and 600 nm in the 40 s etched sample. Despite the Cd depletion, the surface layer still contained significant amounts of Cd; even in the outermost surface layer the Cd/Te ratio was roughly about 2/3 of its bulk value (Fig. 1). This is in a good agreement with the previous X-ray photoelectron spectroscopy (XPS) analysis indicating a Cd/Te ratio of 0.65 on the surface [10]. In addition, about 20 at.% oxygen was found with XPS on the surface of the etch treated film [10].

XRD patterns of unetched and etched samples are compared in Fig. 2. The only discernable difference is the appearance of crystalline, hexagonal tellurium in the etched sample. Together with the SIMS depth profiling results this implies that the etching procedure results in a formation of a surface layer which contains crystalline elemental tellurium. As the presence of Cd (Fig. 1) indicates the surface layer is not pure Te but contains also other phases, most probably CdTe and oxides of Cd and Te.

In the incompletely etched samples the intensities of tellurium XRD reflections were only about one thirds of those in the samples etched normally. In addition, though some variations existed between various samples, the tellurium crystallite sizes estimated from XRD peak broadening using the Scherrer's equation [11] were found to be somewhat smaller in the incompletely etched samples (10–14 nm) than in the samples undergone

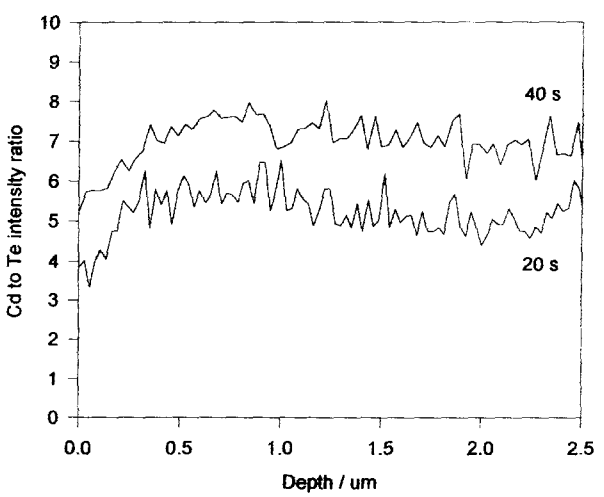

Fig. 1. Cd to Te intensity ratio (SIMS) depth profiles in CdTe films etched in a standard manner for 20 and 40 s. For clarity, the curve for the 20 s etched sample has been shifted down by one unity.

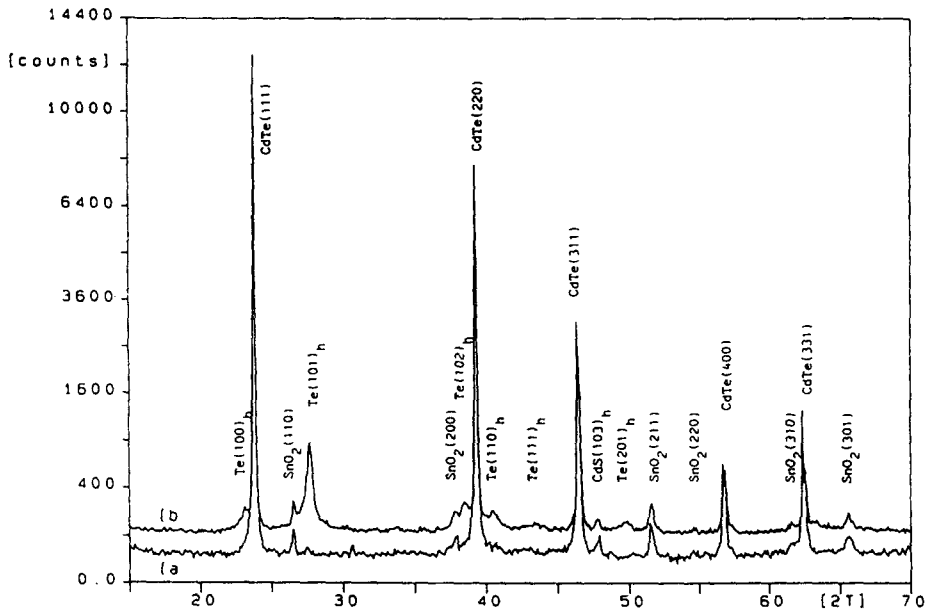

Fig. 2. XRD patterns of (a) an unetched sample and (b) a sample undergone the standard etching procedure.

the normal etching procedure (about 16 nm). When these results are correlated with the above mentioned sheet resistances, it becomes evident that elemental tellurium is responsible for the conductive surface layer. However, even though annealing improved the conductivity of the incompletely etched samples, it did not cause any major changes in either the intensities or widths of the Te XRD peaks. It should be noted, however, that since a Bragg–Brentano geometry, i.e., the θ–2θ geometry, was employed in the XRD measurements the peak broadening gives information only about the crystallite size perpendicular to the film surface. Therefore, it is possible that the heat treatment increases the crystallite size parallel to the film surface thereby increasing the conductivity in that direction.

The sheet resistances measured for the 20 and 40 s etched samples shown in Fig. 1 were 100 and 53 $\Omega/\square$, respectively. Using the surface layer thicknesses estimated above, resistivities of about 3 Ωcm were evaluated from these sheet resistances. This resistivity is somewhat higher than those, 0.1–0.5 Ωcm [12], reported for pure evaporated Te thin films which is evidently due to the fact that the surface layer formed by etching is not a single phase Te. Therefore, it is more meaningful to compare the present results with the diphasic $(CdTe)_{1-x}Te_x$ films deposited by flash evaporation [13]. At low Te contents the resistivities of these films were around 10^8 Ωcm, but when x in $(CdTe)_{1-x}Te_x$ increased to 0.4 the resistivity exhibited a rapid decrease to about 100 Ωcm and finally reached a saturation level of about 1 Ωcm, i.e., close to the value estimated in the present study for the surface layer. These results were interpreted by a percolation conductivity mechanism where Te is the conducting phase [13]. Obviously, this interpretation applies to the present case as well.

3.3. Effect of etching time

To find the optimum conditions for a reproducible etching procedure, the stabilized sheet resistances and Te XRD intensities were studied as a function of the etching time (Fig. 3). The intensity of the Te XRD reflection increases steadily along with the etching time without any tendency towards saturation. The sheet resistance, in turn, shows initially a sharp decrease at etching times less than 30 s after which the decreasing rate slows down. The value of 200 kΩ/□ shown in Fig. 3 for 10 s etching time represents only the most typical sheet resistance measured; in some areas the sheet resistances were as high as 7700 kΩ/□. Such a strong variation is indicative of inhomogeneities in this particular sample. Already in the sample etched for 20 s the variation range decreased significantly and the sheet resistances were within a range of 84–102 kΩ/□.

When the etching time exceeded 80 s the sample became destroyed in a way that part of the surface layers flaked off during washing in an ultrasonic bath. In fact, some small locally damaged areas were observed already in a sample etched for 70 s.

3.4. Post etching crystallization and evolution of conductivity

To verify further the correlation between the conductivity and crystalline tellurium, and to identify the reason for that the sheet resistances saturated only after a certain period, the development of XRD intensities and surface resistances were followed as a function of time after taking the samples out of the etching solutions. The XRD intensities were measured at the peak position of the most intense tellurium peak, i.e.,

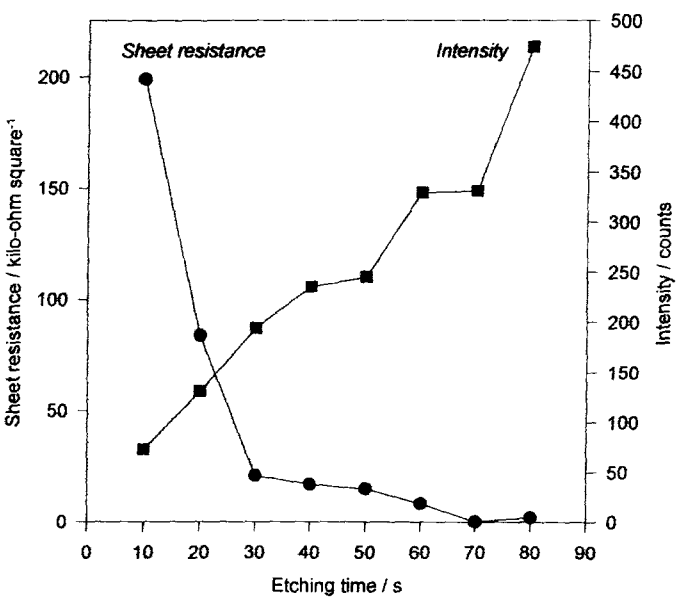

Fig. 3. Sheet resistances and integrated Te(101) XRD intensities as a function of etching time in a standard etching solution.

Te(101) at $2\theta = 27.630°$. The surface resistances were measured with the measuring system described in the experimental section. Thus, instead of being exact sheet resistances, the values given have to be considered only as resistances measured with

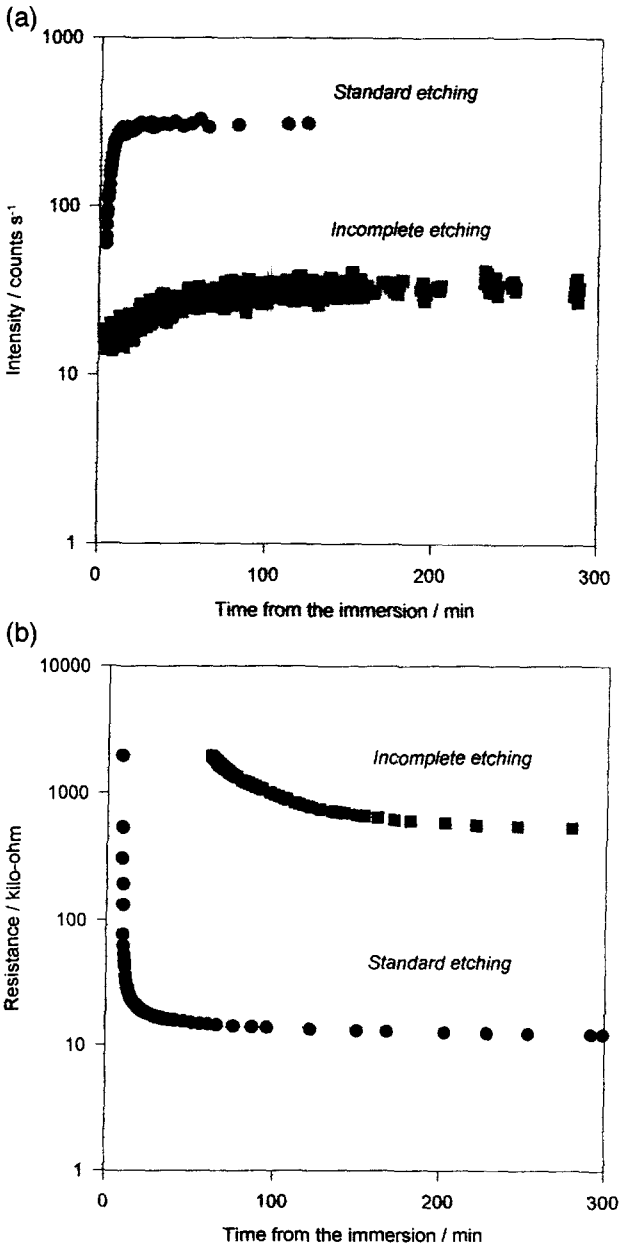

Fig. 4. The development of (a) Te(101) XRD peak heights and (b) surface resistances after standard and incomplete etching procedures. The time is measured from the beginning of the immersion.

this specific instrument and, for clarity, are referred to as surface resistances. Nevertheless, as it has already been pointed out these resistances bear a good log–log correlation to the sheet resistances and, thus, can be reliably employed in following changes which occur in a scale of orders of magnitude.

Fig. 4 depicts the XRD intensity and the surface resistance as a function of time for samples treated with the standard and incomplete etching procedures. The resistances could be measured only when they decreased below 2000 kΩ which is the upper limit for the ohmmeter used in the measuring bench. Clearly, there exists an inverted relationship between the surface resistance and the XRD intensity which reach their saturation levels at the same time. In the case of the standard etching the saturation takes place more rapidly than in the incomplete etching. Furthermore, as was already observed above, the final resistance is lower and the XRD intensity higher in the sample undergone the standard etching procedure. An obvious conclusion from Fig. 4 is that the tellurium is only weakly crystalline immediately after taking out of the etching solution; its crystallization accompanied with the decrease of the surface resistance takes place mainly afterwards.

Fig. 5 depicts how the resistances changed as a function of time when the samples were placed in an oven at 110°C. Comparison of Fig. 5 with Fig. 4b shows that the decrease of the surface resistance was accelerated in a greater extent in the incompletely etched sample than in the sample etched in a standard manner. Unfortunately, no in situ XRD measurements could be performed at 110°C. Nevertheless, XRD measurements carried out from these particular samples after annealing revealed that the integrated intensity of the Te(101) peak was three times higher in the sample undergone the standard etching procedure than in the incompletely etched sample. Also the crystallite

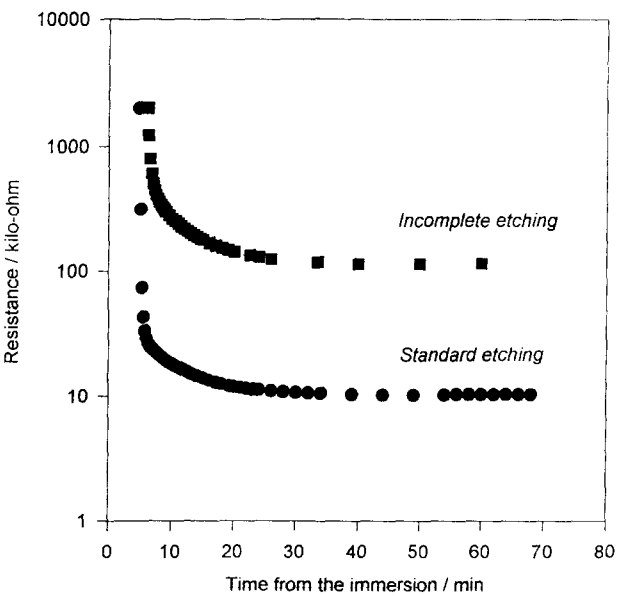

Fig. 5. The development of surface resistances for samples heated at 110°C in air after standard and incomplete etching procedures. The time is measured from the beginning of the immersion.

size was higher in the sample etched in a standard manner (17 nm versus 12 nm). Finally, it should be noted that if the heating time was elongated further the resistance started to increase which is obviously due to the oxidation of Te.

3.5. Alternative etching solutions

In addition to the standard etching solution considered so far, alternative etches derived either by varying the concentrations in the HNO_3–H_3PO_4–H_2O system or by changing one of the etch components were studied as well. In an attempt to slow down the etching reactions for their better control, the standard etching solution was diluted with water. Already after a dilution in a volume ratio 1:1 (standard etch:H_2O), the etching reactions became so slow that even after etching for 7 h the lowest sheet resistance measured was as high as 7.1 M$\Omega/\square$. No evolution of gas bubbles was observed.

To gain further insight into the roles of HNO_3 and H_3PO_4, the etching was performed with solutions which contained only one of the two acids, the volume of the other one being replaced with water. In both cases no discernable changes took place, thereby demonstrating that the both acids have their own important roles in the standard etching solution. Since the main component H_3PO_4 does not possess such a strong oxidizing power as the minor component HNO_3, it seems evident that the role of HNO_3 is to act as an oxidizing agent in a reaction where Te is formed from CdTe, and that H_3PO_4 is mainly acting as a proton source to provide conditions which are acidic enough to favour the reactions leading to the desired products.

In order to verify the role of HNO_3 as an oxidizer it was replaced with another oxidizing agent, hydrogen peroxide (H_2O_2). Etching solutions consisting of 30% H_2O_2, 85% H_3PO_4 and H_2O in volume ratios 1:71:29 (dilute H_2O_2 etch) and 1:33:13 (concentrated H_2O_2 etch) were used. By contrast to the standard etching solution, no silvery surfaces were formed in these etches. Instead, the final film surfaces consisted of black, grey and brown areas. Nevertheless, XRD measurements revealed that hexagonal Te was present also in these samples. Furthermore, the sheet resistances were comparable to those obtained with the standard etching solutions: 27–39 k$\Omega/\square$ for the dilute H_2O_2 etch and 0.95–56 k$\Omega/\square$ for the concentrated H_2O_2 etch. No further attempt was made to identify the reason for the different colour or to optimize the etching conditions.

The replacement of H_3PO_4 with other acids was studied as well. Etching with solutions consisting of acetic acid (CH_3COOH), HNO_3 and H_2O resulted in crystalline Te and sheet resistances as low as 24 k$\Omega/\square$. It was also observed that when the concentration of HNO_3 was kept constant, the sheet resistance was lower the higher the CH_3COOH concentration was. The lowest sheet resistances were obtained with an etch which was made of 65% HNO_3 and 100% CH_3COOH in a volume ratio 1:100. In contrast to the samples undergone the standard etching procedure but parallel to those etched with H_2O_2–H_3PO_4–H_2O mixtures, the surfaces of the samples etched with the HNO_3–CH_3COOH–H_2O solutions consisted of mixtures of black, brown and grey areas.

Attempts to use HCl in place of H_3PO_4 resulted in uneven etching, partial flaking of the film and formation of $CdTeO_3$. When etched with HNO_3–H_2SO_4–H_2O mixtures, after immersion of about 240 s the samples changed their colour to silvery and the

bubbling began. However, when the etching proceeded further, the colour changed back to dark grey. With XRD Te and $CdTeO_3$ were detected as new phases. Since Te is soluble to H_2SO_4, the back and forth change of colour can be attributed to a formation of Te and its subsequent dissolution. The formation of $CdTeO_3$, in turn, may be ascribed to the more powerful oxidizing properties of H_2SO_4 as compared with H_3PO_4.

4. Discussion

The above results clearly illustrate that etching of CdTe film with the HNO_3–H_3PO_4–H_2O mixture produces a Te rich surface layer which contains hexagonal Te as a new crystalline phase. The formation of this surface layer can be divided into three steps. During etching itself there is first a certain induction period, followed by a second reaction step resulting in a formation of the Te rich surface and liberation of gaseous byproducts. Immediately after its formation the Te layer is amorphous; its crystallization accompanied with a substantial decrease of the sheet resistance constitutes the third step of the overall process. To gain a thorough understanding of the etching procedure and, thereby, a better control over it, all these steps should be understood in detail.

4.1. Induction period

Immediately after immersion into the etching solution no changes detectable with an optical microscope, four point resistivity measurements or XRD took place on the CdTe sample surface. The termination of the induction period could be detected from the formation of gas bubbles at the surface, followed almost immediately by a colour change from dark grey to silvery. Importantly, the length of the induction period varied from sample to sample which suggests that this step may be a potential cause for the reproducibility problems of the overall etching procedure.

Because CdTe surface is known to oxidize in air [14,15] it is logical to relate the induction period to the dissolution of the oxide layer. Under acidic conditions TeO_2 is less soluble than CdO and its solubility increases strongly with decreasing pH [16] giving a possible explanation for the importance of high H_3PO_4 concentration, i.e., for having highly acidic etching solution. Variations in sample histories, e.g., in high temperature exposures to air and storage times, can cause differences in the thicknesses of the oxidized surface layers and, thereby, differences in the lengths of their dissolution periods. Further studies on samples with exactly controlled histories are still needed to find the main reason for these variations. Anyhow, in respect of the process control it seems to be sufficient to simply follow either the appearance of the bubbles or the colour change which clearly indicate the completion of the induction period. On the other hand, if etching is to be performed as a large batch process, one has to make sure that all the samples have similar histories.

4.2. Formation of a Te-rich surface layer

The depletion of Cd^{2+} from the surface layer is easily understood by its higher solubility to acidic solutions as compared with Te. The formation of elemental Te, in

turn, requires oxidation since in CdTe the formal oxidation state of tellurium is -II. As the bubbling implies, the oxidation reaction liberates gaseous byproducts. In the standard HNO_3–H_3PO_4–H_2O etching solution HNO_3 is evidently the oxidizing component. The composition of the etching solution was estimated with thermodynamic equilibrium calculations [17], simplified with an assumption that all the activity coefficients are equal to one. According to these calculations at equilibrium the proton concentration $c(H^+) = 7.3$ mol dm^{-3} is so high that a considerable fraction of nitric acid remains protonated; the NO_3^-(aq) to HNO_3(aq) ratio was only about two. Therefore, both HNO_3 and NO_3^- have to be considered as the oxidizing species and the following reactions can be proposed for the oxidation of Te^{2-} to Te^0 accompanied by a dissolution of Cd^{2+} [17]:

$$3CdTe(s) + 8HNO_3(aq) \rightarrow 3Te(s) + 3Cd(NO_3)_2(aq) + 2NO(g) + 4H_2O,$$
$$\Delta G(25°C) = -488\text{kJ/mol}, \quad (1)$$

$$3CdTe(s) + 8H^+(aq) + 8NO_3^-(aq) \rightarrow 3Te(s) + 3Cd(NO_3)_2(aq) + 2NO(g) + 4H_2O, \Delta G(25°C) = -507\text{kJ/mol}, \quad (2)$$

$$CdTe(s) + 4HNO_3(aq) \rightarrow Te(s) + Cd(NO_3)_2(aq) + 2NO_2(g) + 2H_2O,$$
$$\Delta G(25°C) = -128\text{kJ/mol}, \quad (3)$$

$$CdTe(s) + 4H^+(aq) + 4NO_3^-(aq) \rightarrow Te(s) + Cd(NO_3)_2(aq) + 2NO_2(g) + 2H_2O, \Delta G(25°C) = -137\text{kJ/mol}. \quad (4)$$

As the ΔG values indicate all the reactions are thermodynamically feasible. The liberation of NO(g) or NO_2(g) accounts for the experimental observation of bubbling.

In absence of oxidizing species Te^0(s) is the most stable form of tellurium in aqueous solutions at pH = 0 [18]. However, in the presence of HNO_3(aq) or NO_3^-(aq) the oxidation of Te^0(s) to TeO_2(s) is a thermodynamically favoured reaction, e.g., [17]:

$$Te(s) + 4H^+(aq) + 4NO_3^-(aq) \rightarrow TeO_2(s) + 4NO_2(g) + 2H_2O,$$
$$\Delta G(25°C) = -103\text{kJ/mol}. \quad (5)$$

Nevertheless, because of the solubility of TeO_2 into acidic solutions, no TeO_2 layer is formed on CdTe. The fact that a relatively thick layer of Te is formed in the course of the etching process suggests that the further oxidation of Te is slow in comparison with the reactions 1–4. In other words, though thermodynamically favourable, the oxidation of Te^0(s) to TeO_2(s) or Te^{4+}(aq) is kinetically retarded.

The structure and properties of the resulting surface layer depend on the etching time. As the etching time is increased, the volume of Te^0(s) increases steadily as is seen from a constant increase of the intensities of the XRD reflections arising from Te (Fig. 3). On the other hand sheet resistance, being dependent on the lateral continuity and inverse thickness of the Te layer, exhibits a sharp initial drop after which a further elongation of the etching time has only a minor contribution to the total decrease of the sheet resistance (Fig. 3). The third aspect related to the etching time is that if it is increased

too long the sample becomes damaged. Thus, the lower limit of the etching time is dictated by the achievement of the low, nearly stabilized sheet resistance while the upper limit is set by the sample damage. To avoid variations between different samples it is important to measure the etching time from the onset of bubbling, not from the immersion of the sample. According to the present results, the optimum etching time after the appearance of the bubbles is 30–50 s. It should be noted that while determining these etching times only the sheet resistances were considered whereas the performance of the solar cells is affected by the contact resistance through the p-CdTe/Te/metal structure. Nevertheless, it has been verified that the above mentioned optimum etching times are in good accordance with those evaluated from the cell performances [10].

According to the SIMS depth profile (Fig. 1) there is no sharp interface between the surface layer containing elemental Te and the underlying CdTe film. Even though surface roughness apparently has its own spreading effect on the depth profiles, it is still evident that there is a graded interface between Te and CdTe. This kind of a graded interface may explain the uniqueness of the Te layer originating from the etching procedure in forming a low resistance contact to CdTe. Tyan [5] already pointed out that a contact made by vacuum depositing a Te layer on nontreated CdTe surface is inferior to that made by etching.

4.3. Crystallization of Te

The final step in the overall etching procedure is the crystallization of the amorphous Te which acts as an intermediate etching product. Because amorphous Te is an unstable phase at room temperature [19–21] it starts to crystallize immediately after its formation. At room temperature the crystallization is completed within 15 min in the samples etched in a standard manner but a longer time is needed if the etching time has been too short, i.e., in the incompletely etched samples.

Since the resistivity of the crystalline tellurium is about four orders of magnitude lower than that of the amorphous tellurium [22] the crystallization improves remarkably the electrical conductivity of the surface layer. An unfortunate consequence of this relation between crystallinity and conductivity is that the slow crystallization prevents a use of electrical measurements in immediate verification of a successful etching procedure.

The crystallization can be accelerated by a heat treatment which increases the mobility of Te atoms. The effect of the heat treatment is especially pronounced if the etching time has been too short; in that case the heat treatment not only accelerates the crystallization but also lowers the final sheet resistances which is attributed to an improved crystal quality and/or increased crystallite size in a direction parallel with the surface.

5. Conclusions

Etching of CdTe thin films with a HNO_3–H_3PO_4–H_2O mixture produces a Te rich surface layer containing crystalline elemental Te. The formation of this layer takes place

in three steps: (i) dissolution of an oxidized CdTe surface layer, (ii) oxidation of Te^{2-} ion in CdTe to elemental Te, accompanied by a dissolution of Cd^{2+}, and (iii) crystallization of Te causing a marked decrease in the sheet resistance. The last step takes place mainly after the sample has been taken out of the etching solution.

Substantial variations exist in the time needed to complete the first step in different samples, thereby causing reproducibility problems. These problems can be avoided by controlling only the length of the second step, the onset of which can be observed from an appearance of gas bubbles or from a colour change of the surface. On the other hand, if large batches are etched simultaneously all the samples have to possess similar histories to ensure that the thicknesses of the oxidized surface layers are identical.

In the standard HNO_3–H_3PO_4–H_2O etching solution the minor component HNO_3 acts as an oxidizing agent in formation of Te^0 from Te^{2-} whereas the role of H_3PO_4 is to provide conditions which are acidic enough to favour the desired reactions. The most probable reason for the need of having pH close to zero is the low solubility of TeO_2 which increases with decreasing pH. The etching reactions become retarded to an unpractically low level already when the etching solution is diluted in a 1:1 ratio with water. On the other hand, the both acids in the standard etching solution can be replaced with other reagents possessing parallel characteristics, i.e., H_2O_2 can be used as an oxidizing agent in place of HNO_3, and the pH can be adjusted with CH_3COOH instead of H_3PO_4.

Acknowledgements

Mr. Pekka Tarkiainen is appreciated for constructing the in situ resistance measuring bench. A scholarship for JS from Microchemistry Ltd is gratefully acknowledged.

References

[1] K. Zweibel, T.L. Chu and S.S. Chu, Adv. Sol. Energy 8 (1993) 271.
[2] T. Suntola, MRS Bull. Oct. (1993) 45.
[3] A.L. Fahrenbruch, Solar Cells 21 (1987) 399.
[4] R.H. Bube, Annu. Rev. Mater. Sci. 20 (1990) 19.
[5] Y.-S. Tyan, US Patent 4,319,069 (1982).
[6] A. Rautiainen, Y. Koskinen, J. Skarp and S. Lindfors, Mat. Res. Soc. Symp. Proc. 222 (1991) 263.
[7] A. Kytökivi, Y. Koskinen, A. Rautiainen and J. Skarp, Mat. Res. Soc. Symp. Proc. 222 (1991) 269.
[8] P.V. Meyers, C.H. Liu and T.J. Frey, US Patent 4,710,589 (1987)
[9] S.A. Ringel, A.W. Smith, M.H. MacDougal and A. Rohatgi, J. Appl. Phys. 70 (1991) 881.
[10] E. Siponmaa, J. Sarlund, M. Ritala and M. Leskelä, Proc. 13th Eur. Photovoltaic Solar Energy Conf. (Nice, 1995).
[11] A. Segmüller and M. Murakami, in: K.J. Klabunde (Ed.), Thin Films from Free Atoms and Particles (Academic Press, Orlando, FL, 1985) p. 325.
[12] M.A. Dinno, M. Schwartz and B. Giammara, J. Appl. Phys. 45 (1974) 3328.
[13] R. Ramírez-Bon, F.J. Espinoza-Beltrán, M. Pedroza-Montero, F. Ruíz, J. González-Hernández, O. Zelaya-Angel and F. Sánchez-Sinencio, Appl. Phys. Lett. 65 (1994) 3254.
[14] J.G. Werthen, J.-P. Häring and R.H. Bube, J. Appl. Phys. 54 (1983) 1159.
[15] S.S. Choi and G. Lucovsky, J. Vac. Sci. Technol. B6 (1988) 1198.

[16] D.E. Aspnes and H. Arwin, J. Vac. Sci. Technol. A2 (1984) 1309.
[17] Outokumpu HSC Chemistry for Windows program package, Version 1.10 (Outokumpu Research Oy, Pori, Finland, 1993).
[18] R.B. Heslop and P.L. Robinson, Inorganic Chemistry, 3rd ed. (Elsevier Science, Amsterdam, 1967) p. 470.
[19] J. Feinleib and S.R. Ovshinsky, J. Non.-Cryst. Solids 4 (1970) 564.
[20] W.-Y. Lee, H. Coufal, C.R. Davis, V. Jipson, G. Lim, W. Parrish, F. Sequeda and R.E. Davis, J. Vac. Sci. Technol. A4 (1986) 2988.
[21] Y.-S. Tyan, D.R. Preuss, F. Vazan and S.J. Marino, J. Appl. Phys. 59 (1986) 716.
[22] J. Stuke, J. Non-Cryst. Solids 4 (1970) 1.